LONGITUDINAL PHASE SPACE CHARACTERIZATION AT FERMI@ELETTRA[#]

E. Ferrari* Elettra - Sincrotrone Trieste and Universita' degli Studi di Trieste, Italy
E. Allaria, P. Cinquegrana, M. Ferianis, L. Froelich, L. Giannessi, G. Penco,
M. Predonzani, F. Rossi, P. Sigalotti, M. Veronese, Elettra - Sincrotrone Trieste, Italy

Abstract

The seeded FEL FERMI@Elettra has completed the commissioning of FEL-1 line, and it is now providing the User Community with a coherent and tunable UV radiation (from 70 nm to 20 nm) in a number of different configurations, including an original twin-seeded pump-probe scheme. Among the key sub systems for the operation of FERMI@Elettra, there are the femtosecond optical timing system, some dedicated longitudinal diagnostics, specifically developed for FERMI@Elettra and, of course, state of art laser systems. In this paper, after a short review of the FERMI@Elettra optical timing system and of its routinely achieved performances, we focus on the results obtained from the suite of longitudinal diagnostics (Bunch Arrival Monitor, Electro Optical sampling station and RF deflectors) all operating in single shot and with 10s fs resolution which demonstrate the FERMI@Elettra achieved performances. The results from these longitudinal diagnostics are compared and shot to shot correlated with the results obtained from an independent longitudinal measurement technique, based on a spectrometer measurement of a linearly chirped electron bunch, which further validate the FERMI@Elettra operation.

INTRODUCTION

FERMI free electron laser (FEL) is a fourth generation light source located at Elettra - Sincrotrone Trieste laboratory, Italy [1]. It has been designed as a user facility and to produce photons in the ultraviolet and soft X-ray wavelength regions. The scientific case, based on three experimental programs, namely Diffraction and Projection Imaging (DiProI), Elastic and Inelastic Scattering (EIS), Low Density Matter (LDM), calls for stable, high peak brightness, nearly fully coherent, narrow bandwidth photon pulses, together with wavelength tunability and variable polarization [2, 3].

FERMI is a seeded FEL based on the high gain harmonic generation (HGHG) scheme [4]. Two FEL lines are presently installed at the facility, FEL-1 and FEL-2. FEL-1 is a single stage cascaded seeded FEL and it is capable of generating coherent light in the 65-20 nm wavelength range. FEL-2 is a double stage seeded FEL based on the "fresh bunch injection" technique [5], where the additional stage extends the frequency up-conversion to the spectral range of 20-4 nm. The FEL-1 beam line is in operation since the end of 2010, with user experiments carried on in 2011-2013 and user beam time allocated until the first half of 2014. FEL-2 is actually in commissioning phase.

The HGHG scheme is based on the interaction of an external laser (usually in the UV spectral range) with a relativistic electron beam in a short undulator (modulator). The interaction induces energy modulation, which is then converted into a density modulation (bunching) by letting the electron beam pass through a short dispersive section. Such a modulated beam can produce coherent radiation when injected into a long undulator (radiator), tuned to one of the harmonics of the seed laser. The emission produced in this way can be amplified through the FEL process. In this configuration is possible to produce FEL pulses characterized by a good transverse and longitudianl coherence, much higher than what is possible with SASE schemes [6].

The electron bunch needed for FERMI operations is provided by a single-bunch, S-band high brightness electron linac. The linac is presently capable of reaching a final energy up to 1.4 GeV in FEL operative conditions.

One of the key systems of the accelerator is the timing system. The system is in charge of the generation and distribution, with femtosecond accuracy, of the phase reference signal to all the time critical accelerator systems and of the machine trigger [7]. The measured phase noise of the phase reference signal, as delivered to the various end stations, is typically <20 fs (rms). For a complete description of the FERMI timing system one can refer to [8].

In this Paper we present the experimental results obtained on the longitudinal diagnostics present in the machine, as well as the calibration procedures we performed for validating the findings and the shot-by-shot comparison between each of the devices.

LONGITUDINAL DIAGNOSTICS

The FERMI machine scheme is reported in Fig.1 with the LINAC (top), undulator hall (center) and experimental hall (bottom). Electron extracted from a photo-injector (PIL and GUN) at 6 MeV are accelerated up to 1.2 / 1.4 GeV at the linac end. The bunch length can be manipulated by means of a magnetic bunch compressor chicane (BC1). Also, just before BC1 there is the laser heater (LH) system. After the acceleration, the electrons are injected into one of the two FEL lines (FEL-1 and FEL-2), where the FEL radiation is produced. The electron bunch length along the machine varies from less than 10 ps out of the injector to

* eugenio.ferrari@elettra.eu.

[#]This work has been supported in part by the Italian Ministry of University and Research under grants FIRB-RBAP045JF2 and FIRB-RBAP06AWK3.

ISBN 978-3-95450-127-4

1 ps or less after compression, hence the diagnostics have been optimized for different beam regimes.

Along the whole machine a series of longitudinal diagnostics are present. After BC01 there is a Bunch Arrival Monitor (BAM) and an RF-deflector (1 in Fig.1), which are used to characterize the bunch properties in the low energy part of the machine. At the linac end (2) there are two RF-deflectors and a dipole spectrometer (DBD, 3). Then, at the beginning of both the FEL lines (4) there is another BAM and the Electro Optical Sampling (EOS) station. At the end of the undulator hall, just before the main beam dump (5) another electron energy spectrometer has been installed.

In the case of an FEL in general, and of FERMI in particular, the beam properties one is interested in are both the whole beam ones (emittance, energy, sizes, etc.), as well as the ones of small longitudinal "slices" of the beam itself. This is because the FEL process happens, in a seeded FEL, only in the part of the electron beam which interacts with the seed laser itself, that is usually <200 fs long[1]. Typical longitudinal measurements performed during FERMI operations are slice beam energy, energy spread and energy chirp, current distribution, bunch length, arrival time jitter, etc. Some of the measurements are destructive, while others can be performed on line shot-by-shot and can therefore be used to stabilize the electron beam properties using dedicated feedback loops. In the following we will focus on the performance of each of the different longitudinal diagnostics installed at FERMI.

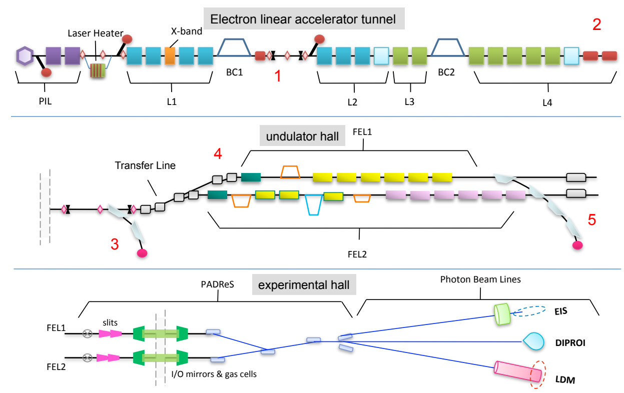

Figure 1: FERMI machine setup, with the linac tunnel (top), undulator hall (center) and experimental hall (bottom). Electron extracted from a photo-injector (PIL and GUN) at 6 MeV are accelerated up to 1.2 / 1.4 GeV at the linac end. The bunch length can be manipulated by means of a bunch compressor chicane (BC1). Also, just before BC1 there is the laser heater (LH) system. After acceleration the electrons are then transported to one of the two FEL lines (FEL-1 and FEL-2), where the laser radiation is produced. Finally the photons are transported to one of the three experimental stations in the experimental hall. There are many longitudinal diagnostics along the machine. After BC01 (1) there is a Bunch Arrival Monitor (BAM) and an RF deflector, at the linac end (2) two RF deflectors are installed. There is an electron energy diagnostic spectrometer (DBD, 3) located before the undulator hall, another BAM station (4) and an Electro Optical Sampling (EOS) station at the beginning of each undulator chain. Finally, just before the main beam dump (MBD, 5) there is another electron energy spectrometer.

BUNCH ARRIVAL MONITOR (BAM)

The Bunch Arrival Monitor (BAM) developed for FERMI is based on the original idea of the DESY advanced diagnostics group [10]. To operate the BAM on the real beam a coarse and fine time alignment of the electron bunch signal, obtained from the BAM pick-up, to the nearest optical pulse from the stabilized link is needed, as well as a calibration [8]. While the system is auto-calibrated, a cross calibration check has been performed in order to validate the diagnostic. To do that we focused first on the BC01 BAM (cfr. Fig.1, (1)) and correlate the BAM readings with the ones of a time-calibrated BPM located at the center of the chicane, while we artificially inducing a sinusoidal change (with increasing amplitude) in the time of flight of the electron beam through the chicane itself. This is done by changing the reference of a dedicated feedback, which in normal operations is used to keep the beam properties as stable as possible during compression, while recording shot-to-shot the arrival time at the BAM and the calibrated BPM position.

In Fig.2 the obtained results for the calibration are presented. In the left panel both the BPM and BAM readings are reported as a function of the shot number, in the right panel the analysis of the correlations between the two devices is presented. The correlation coefficient is larger

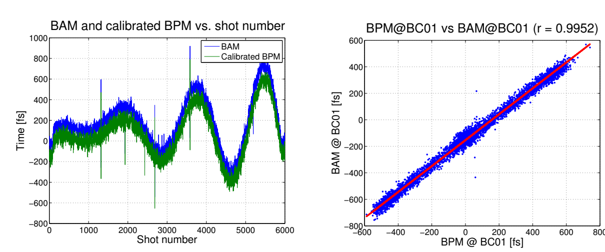

Figure 2: BAM calibration using the BPM in the BC01 chicane. The time-of-flight through the chicane has been changed by artificially inducing a sinusoidal perturbation with increasing amplitude. Left panel: BAM and BPM arrival time variation (in fs) as a function of the shot number. Right panel: Correlation between the two devices. The correlation coefficient shows an agreement of more than 99%.

[1] In the case of SASE, the FEL process happens on parts of the beam of the order of the cooperation length [9].

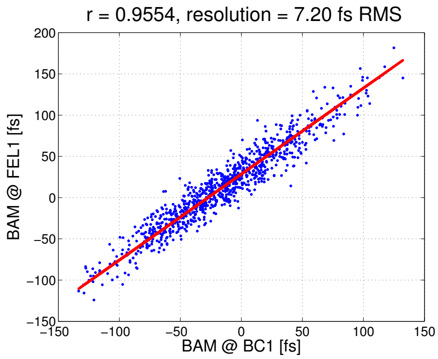

Figure 3: Estimation of the BAM resolution. By looking at the width of the the shot-to-shot correlations between the BC01 BAM (1 in Fig.1) and the FEL-1 BAM (4) we are able to have an upper estimation of the resolution of each of the two devices, which is less than 8 fs (rms). Arrival time variations in the accelerating cavities in between the two BAMs have been neglected.

than 99%, which is a clear indication of the accuracy of the BAM self-calibration process.

After having checked that the BAM calibration was adequate, we tried to estimate an upper limit for the resolution of the device. To do that we analyzed the shot-to-shot correlations between the BC01 BAM (1 in Fig.1) and the FEL-1 BAM (4). In Fig.3 we report the results obtained for 1000 shots. The width of the distribution is in fact (mainly) due to the resolution of the instruments, that for simplicity is considered the same for both pick-ups. If we also neglect the possible contributions to time jitter due to the accelerating sections in between the two devices, we can have an upper estimation of the resolution of the BAMs, which in the FERMI case turns out to be less than 8 fs. These assumptions are reasonable as the correlation coefficient is always $> 95\%$. BAMs represent the reference arrival time diagnostic for FERMI and are routinely used to investigate time jitter sources. Typical values for the arrival time jitter are ~60 fs (rms) after the BC01 chicane and ~70 fs (rms) at the beginning of the FEL-1 line.

RF DEFLECTORS

FERMI is equipped with three RF-deflecting cavities [11], one is located after the first bunch compressor (1, in Fig.1) and two at the linac end (2). An RF-deflector is used to give a longitudinal kick to the electron beam that depends linearly on the arrival time at the cavity. Depending on the kick direction and after proper calibration, the vertical (horizontal) coordinate at a downstream screen is mapped to the time variable and the longitudinal beam properties can be diagnosed. Routine measurements include bunch length, current distribution, slice emittance, etc.

As already presented in the BAM section, we were able to check the calibration of the arrival time variations by artificially change the time-of-flight in the BC01 chicane.

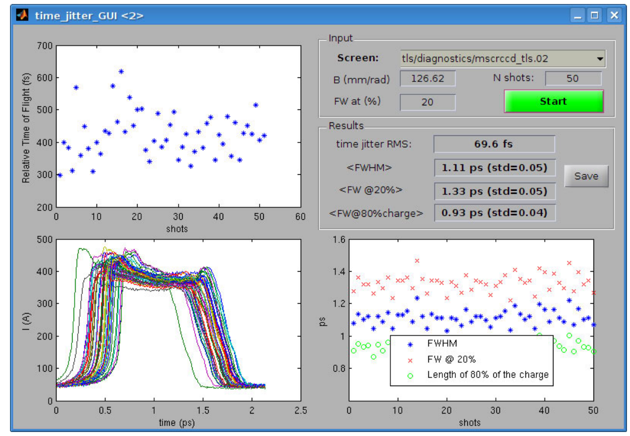

Figure 4: Measurement of the time jitter at linac end, using the high energy RF deflector (vertical). The RF deflector is also routinely used for bunch length and current distribution measurements. The estimated time jitter is ~70 fs, in agreement with the results provided by the BAM at the beginning of the undulator chain.

This approach can be also used to check the RF-deflector calibration, compare the results with the BAM and estimate the RF-deflector resolution. In Fig.5 we report the results of the calibration process, for both the BAM and the deflected beam profile at the linac end, as a function of the shot number. The agreement between the two measurements is satisfactory (correlation coefficient ~95%) despite some differences, probably due to slow drifts in the klystron powering the cavity. In this way it is also possible to estimate the resolution of the RF-deflector measurements, which in the FERMI case is of the order of 50 fs (rms).

Electron longitudinal phase space (LPS) can instead be diagnosed by coupling a bending magnet spectrometer (3 in Fig.1, for energy resolution) with an RF-deflector (for time resolution) [12]. An example of the LPS measurement, performed with a dedicated matlab GUI, is reported in Fig.6. Using this diagnostic device one is able to recover the energy chirp along the bunch, the slice energy spread etc, which are valuable quantities for machine optimization and FEL operations. Typical values for the slice energy spread at the LINAC end are less than 150 keV.

ELECTRO OPTICAL SAMPLING (EOS)

At the beginning of each of the FEL lines (cfr. Fig.1) an electro optical sampling (EOS) station [13], based on the spatial encoding scheme [14] is installed. In the following we will focus on the FEL-1 EOS only. The EOS is capable of providing both time jitter and longitudinal profile measurements in a non-destructive way.

In Fig.7 we report the results of the time jitter measurements taken at the EOS station (left panel) and the comparison with the nearby BAM at FEL-1 (right panel). The EOS acquisition is affected by a large noise. If one consider the full data (blue) the measured time jitter is ~250

ISBN 978-3-95450-127-4

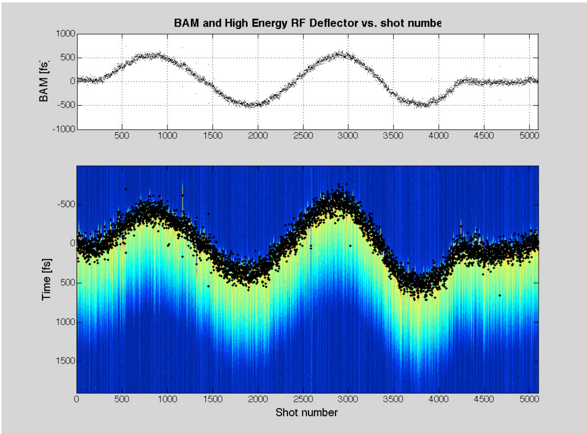

Figure 5: Measurement of the arrival time variation at the linac end, while a sinusoidal perturbation was induced in the BC01 chicane (cfr. BAM cross-calibation description in BAM section). Both the BAM measurement (top) and the deflected beam profile (bottom) are reported, as a function of the shot number. For the profile, the head position is also plotted for an easier comparison with the BAM results. The agreement between the two measurements is satisfactory and the estimated resolution for the RF-deflector is ∼50 fs (rms).

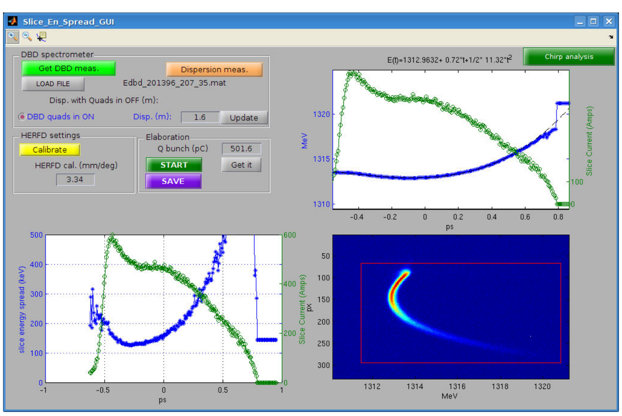

Figure 6: Measurement of the longitudinal phase space at the DBD spectrometer. The longitudinal phase space can be measured by coupling a beam energy spectrometer (horizontal) with an RF deflector (vertical) in order to have both the time and energy distributions of the electrons in the beam. In figure, the matlab GUI used for the post processing of the measure is presented. The scheme is also routinely used for current profile, energy chirp, bunch length and slice energy spread measurements.

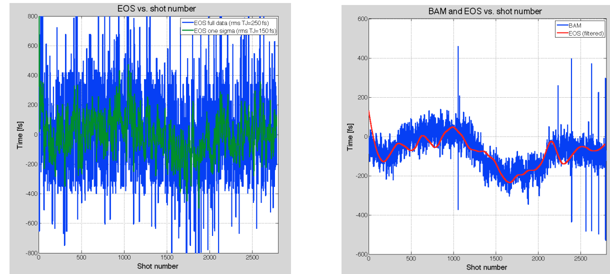

Figure 7: Measurement of arrival time jitter at the EOS station and comparison with the FEL-1 BAM. Left panel: EOS arrival time jitter measurements. If one consider the full data (blue) the time jitter is ∼250 fs (rms), while considering only the shots within 1 σ the value is ∼120 fs (rms). The acquisition is affected by a large noise, probably due to the locking electronics, preventing shot-to-shot correlations. Nevertheless, after adequate filtering of the data (right box, red curve), is possible to observe an agreement with the BAM results (blue line).

fs, while considering only the shots within 1 σ, the value drops to ∼120 fs. This is a first indication that the integration window of the instrument needs to be adjusted in order to be able to record the whole beam. The main source of the measurement noise has been identified in the fiber laser locking, which is undergoing an upgrade and needs to be further tuned.

In the right panel of Fig.7 the EOS data (blue curve) are compared with the BAM (red curve), after a proper filter has been applied: the behavior of the two systems shows a good agreement, which we expect will be there also at the shot-to-shot level.

THE HOLE

In a seeded FEL the interaction between the electron beam and the seed laser modify locally the energy distribution of the electron beam [15]. By taking advantage of the correlation between time and energy in the case of a quasi-linearly chirped electron beam and the fact that the FERMI seed laser pulse is much shorter than the electron beam duration, longitudinal measurements of the e-beam pulse length, local energy chirp and current are possible. After a proper calibration that allows to convert the horizontal coordinate of the MBD images into fs, it is possible to retrieve the relative position between the e-beam and the seed laser in fs and measure the jitter between the two.

Experimental results, reported in Fig.8, clearly show the presence of an hole in the electron beam spectrum when the seed laser is present. By measuring the evolution of the hole in the MBD spectra we can measure the changes in the relative timing between the electron beam and the seed laser for each shot: an example of a series of 200 seeded shots is reported in Fig.9. With this method we are able to measure a jitter of about 70 fs (rms) between the laser and the electron beam.

ISBN 978-3-95450-127-4

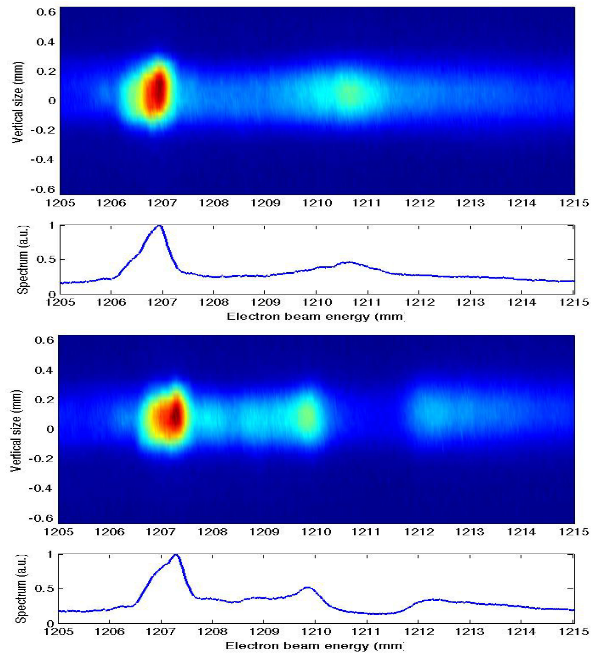

Figure 8: The electron beam energy spectrum in MBD. Top: unseeded case. Bottom: seeded case. In specific configurations of the linac, the electron beam measured at the end of the accelerator shows strong linear time-energy correlation. Experimental results clearly show an hole in the electron beam spectrum as a result of the seeding process.

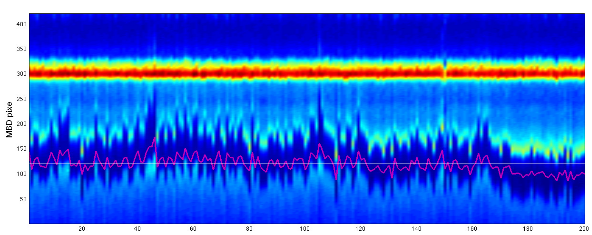

Figure 9: Sequence of 200 seeded electron beam spectra measured in MBD. While the peak is fixed in energy, the position of the seed induced hole is moving. After a proper calibration, it is possible to retrieve the relative position between the e-beam and the seed in fs and measure the jitter between the two, which turns out to be ~70 fs (rms). By measuring the evolution of the hole we can also evaluate the changes in the relative timing between the electron and seed laser for each shot.

CONCLUSIONS AND PROSPECTIVE

We presented the longitudinal diagnostics and measurements performed at FERMI. The instruments are routinely used during FEL commissioning and user experiment and are one of the key components that contribute to FERMI reliability. The diagnostics and feedback systems are capable of keeping the time jitter of the electron beam well under control, with typical values at the undulator line of around 70 fs (rms). Continuous improvements are undergoing, in order to increase the measurement capabilities and to further improve the reliability. A major update for machine operations will be the inclusion of the different longitudinal feedbacks into a single tool. Long term upgrades include the possibility of moving one high energy RF-deflector from the linac end to the undulator chain end, to include the BAMs output in timing feedback loops, to improve the EOS laser for on-line longitudinal beam profile measurements during FEL operations and finally to take advantage of the hole effect as FEL emission diagnostic.

REFERENCES

[1] C. J. Bocchetta et al., “Conceptual Design Report for the FERMI@Elettra project”, ST/F-TN-07/12 (2007).

[2] E. Allaria et al., “Highly coherent and stable pulses from the FERMI seeded free-electron laser in the extreme ultraviolet”, Nat. Phot. **6**, 233 (2012).

[3] E. Allaria et al., “Tunability experiments at the FERMI@Elettra free-electron laser”, New J. Phys. **14**, 113009 (2012).

[4] L.H. Yu, “Generation of intense uv radiation by subharmonically seeded single-pass free-electron lasers”, Phys. Rev. A **44**, 5178-5193 (1991).

[5] I. Ben-Zvi, K.M. Yang, L.H. Yu, “The “fresh-bunch” technique in FELs”, NIM A **318** p726-729 (1992).

[6] Yu et al., “High-Gain Harmonic-Generation Free-Electron Laser”, Science **289** (5481) 932-934 (2000).

[7] M. Ferianis “State of the Art in High-Stability Timing, Phase Reference Distribution and Synchronization Systems”, Proceedings of PAC ’09 Vancouver, BC, Canada (2009).

[8] M. Ferianis et al. “The FERMI copper free timing system: implementation and results” Proceedings of BIW10, Santa Fe, NM, USA (2010).

[9] R. Bonifacio et al., “Physics of the High-Gain FEL and Superradiance”, Riv. Nuovo Cimento, **17**, 9 (1990).

[10] F. Loehl, “Optical Synchronization of a Free Electron Laser with femto-second precision”, Ph.D. Thesis at Hamburg University (2009).

[11] M. Petronio, “Research and Applications of Radio-Frequency Deflecting Cavities”, Ph.D. Thesis at Trieste University (2009).

[12] G. Penco et al., “Time-Sliced Emittance and Energy Spread Measurements at FERMI@Elettra”, WEPD20, Proceedings of FEL2012, Nara, Japan (2012).

[13] M. Veronese et al., “First Operation of the Electro Optical Sampling Diagnostics of the FERMI@Elettra FEL”, TUPA43, Proceedings of IBIC2012, Tsukuba, Japan (2012).

[14] A. Cavalieri et al., “Clocking femtosecond x-rays”, Phys. Rev. Lett. **94** 114801, (2005).

[15] E. Allaria et al., “Measurement of electron-beam and seed laser properties using an energy chirped electron beam”, MOPSO02, Proceedings of FEL2013, New York City, NY, USA (2013).

ISBN 978-3-95450-127-4